

CALIBRATION OF AN ENERGYPLUS SIMULATION OF A PHASE CHANGE MATERIAL PRODUCT USING EXPERIMENTAL TEST CELL DATA

Nathan Brown^{1,2}, Santosh Philip¹, Ibone Santiago Trojaola¹,
Susan Ubbelohde^{1,3}, and George Loisos¹
¹Loisos + Ubbelohde, Alameda, CA
²California College of the Arts, San Francisco, CA
³University of California, Berkeley, Berkeley, CA

ABSTRACT

This paper presents a calibration process for determining an accurate EnergyPlus modeling methodology for a particular Phase Change Material (PCM) product consisting of PCM contained in pouches sandwiched between two sheets of plastic. Two test cells were constructed to control for the effect of the PCM product. Monitored test cell data were used to first calibrate an EnergyPlus model of the control test cell, and then to calibrate the EnergyPlus PCM module for the PCM product under investigation. The study results include calibrated PCM EnergyPlus module values for the PCM product. The results also demonstrate the importance of explicitly modeling heat transfer paths containing PCM separately from those not containing PCM.

INTRODUCTION

Phase Change Materials (PCMs) have the potential to reduce reliance on building mechanical heating and cooling systems, because they can store and release latent heat over time, as has been demonstrated in a variety of experimental and theoretical studies (eg. Silvia et al. 2012, Medina et al. 2008, and Kissock and Limas 2006).

This research was motivated by an initial question about potential energy performance benefits of a particular PCM product on a project. The PCM product is supplied in sheets of plastic that contain arrays of pouches containing PCM (see Figure 1). When we studied the impacts of this PCM product in our EnergyPlus model using the inputs suggested by the manufacturer, we were not able to reproduce impacts comparable to the manufacturer's generic EnergyPlus model. It was not clear whether the inputs or modeling method were accurate. Existing literature did not provide sufficient guidance. Indeed, despite the large volume of recent literature on PCM in buildings, there

is still a lack of confidence in the predicted behavior of PCMs (Dutil et al. 2014).

It has been shown that EnergyPlus can model the behavior of PCM (Pedersen 2007). A recent software update has corrected some flaws in the EnergyPlus PCM algorithms, and verified that PCMs can be modeled with reasonable accuracy (Tabares-Velasco 2012). However, most prior studies have dealt with PCM contained homogeneously with some other material. One study analyzed PCM contained in pouches similar to the product in this study and applied the results to an EnergyPlus model (Kosny 2010). Kosny utilized a process for simplifying complex wall assemblies into a one-dimensional set of layers that substitute for the more complex geometry. However, this study validated its results using full-cycle heating and cooling process, which may not apply when PCM is subject to repeated partial melting and/or freezing. Full melt and freeze cycles may be correct assumptions for PCM located towards the exterior of a wall assembly, but may be problematic given the less widely-varying temperatures typical of interior surfaces, near which has been shown to be a desirable location for enhanced PCM performance (Jin et al 2013).



Figure 1 The PCM product tested in this study

This paper examines the thermal behavior of this particular PCM product, with the goal of identifying an accurate method of modeling its thermal behavior in a building using EnergyPlus.

PHASE CHANGE MATERIAL THERMAL PROPERTIES

GENERIC

For the purposes of accurately modeling the thermal behavior of any PCM, there are a number of properties that must be specified accurately. The essential characteristic of a PCM is the ability to store and release latent heat at an engineered temperature. A number of methods exist for characterizing and modeling the behavior of PCMs (Kuznik et al, 2011). Since the results of this study needed to be integrated in existing EnergyPlus models, we limit the scope of the paper to the inputs and methods used by EnergyPlus.

An enthalpy curve is a common characterization of PCM and a key input for modeling PCMs in EnergyPlus. This curve describes the relationship between the total energy contained in a sample of the material and the corresponding temperature of the material (see figure 2 below). Consider a sample of PCM that starts out at a cold temperature (point 1 in the figure). Increasing enthalpy (adding heat) will at first increase the temperature rapidly (according to its specific heat). At the phase transition temperature (starting at point 2), the material begins to transition from solid to liquid. In the temperature range where this phase change occurs, increasing enthalpy will produce a small increase in temperature. Once the sample is entirely melted (point 3), the temperature will once again increase rapidly as enthalpy increases.

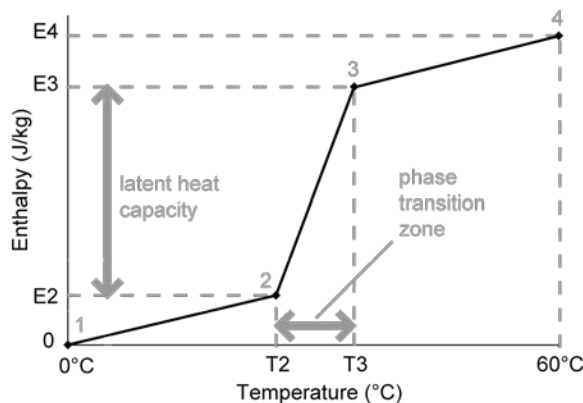


Figure 2 Generic enthalpy curve for phase change material

For the purposes of this study, we define the enthalpy curve according to five essential values. These values allow an enthalpy curve to be established between 0C and 60°C, and assume enthalpy is 0 at 0°C.

- T2, the temperature at which point phase transition begins
- E2, the enthalpy where phase transition begins
- T3, the temperature at which point phase transition ends
- E3, the enthalpy where phase transition ends
- E4, the enthalpy should the temperature reach 60°C

The remaining essential thermal properties determine how the PCM can absorb and release energy. These are:

- thermal conductivity
- thermal conductivity temperature coefficient (determining if the conductivity varies depending on temperature), and
- geometry used to model PCM.

We note that this model does not include representation of hysteresis. For materials that exhibit strong hysteresis, we would expect accuracy of the model to suffer (Tabares-Velasco 2012, Dutil et al. 2014).

PCM PRODUCT

This study investigates the thermal performance of a specific PCM product. The PCM itself is a gel, sandwiched between two sheets of plastic. The PCM is held in small capsules with space in between such that approximately 4/9 of the surface is PCM, while the remaining surface is plastic only. The product is sold in sheets, which can be placed in various locations in building assemblies.

The supplier provides the PCM product in a low, medium, and high capacity (ie, PCM mass) per square foot, and at various phase transition setpoints. The specific product tested in this study is the low capacity product with an expected phase transition temperature of 25°C.

TEST CELL DESIGN AND CONSTRUCTION

Two test cells were constructed identically in order to isolate the thermal behavior of the PCM from the thermal performance of the rest of the test cell construction. An air gap was provided in the test cell enclosure assembly in both the control test cell as well as the PCM test cell; the PCM was placed on one side of the air gap in the PCM test cell. The test cell enclosure assembly was used on all six sides of the test cell (see Figure 3).

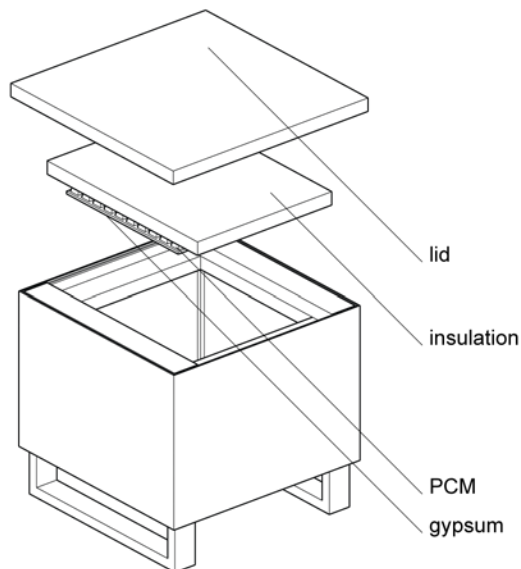


Figure 3 Test cell construction

The test cells were designed in order to be both manageable to work with and also to create conditions that would drive the temperature of the PCM through the phase transition zone within a daily cycle. Ultimately the goal of the larger project was to better model PCM behavior in actual buildings, and so we also designed the test cell assemblies to roughly correspond to assemblies used in buildings.

The test cell dimensions were selected so that one sheet of PCM exactly matched the dimensions of the interior of each wall. Layers of the test cell enclosure assembly were the same for all six sides: painted marine plywood, expanded polystyrene insulation, an air gap (which includes PCM in one test cell), and gypsum. Since the thermal properties of this assembly were critical, an initial EnergyPlus energy simulation was used to ensure that the specific selection of exterior paint reflectivity, insulation thickness, and gypsum thickness would produce temperature variation through the PCM phase transition zone. Initially, a paint reflectivity of 50%, 2 inches of XPS, and 3/8 in. of gypsum were used (See Figure 4). The exterior was subsequently repainted with a darker paint when it was discovered that the PCM was not experiencing temperatures in the upper end of the phase transition zone.

The test cell was constructed to high standards of precision in order to keep the assemblies as thermally consistent as possible. To minimize the risk for unanticipated air gaps, marine plywood was selected for

the exterior, and all insulation was cut to precise lengths. Vertical joints were made efficiently using a lock miter joint, and the base was constructed with a dado joint. The top edges of the sides were finished with weather stripping, resulting in a box with virtually no infiltration. All interior edges of the box were filled with 4 in. square pieces of expanded polystyrene, and panels of insulation, PCM, and gypsum were held in place using upholstery pins to avoid thermal bridging created by fasteners and to allow the boxes to be reconfigured quickly.

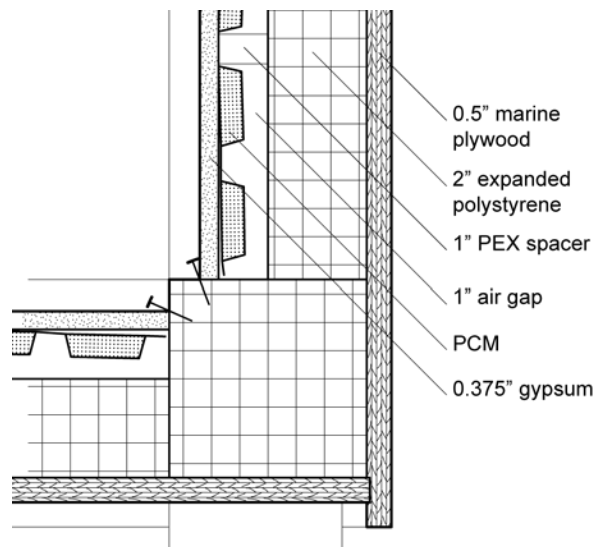


Figure 4 Test cell construction detail

We also installed systems to regulate the interior temperatures of the test cells if needed. For each test cell, an identical system was used. This system consisted of a single water loop running between an external auxiliary box and the test cell. In the auxiliary box, the loop contained a pump, an aquarium chiller, and an aquarium heater. The loop then continued in an insulated and shielded supply line to the test cell, where it connected to a water to air heat exchanger (we used an automotive heater core with a muffin fan), and then returned to complete the loop in the auxiliary box (see Figure 5).

MONITORING

The test cells were placed in full sun, oriented the same way, and then monitored in order to quantify their thermal performance (See Figure 6). We installed a variety of monitoring equipment to characterize the test cell performance. The primary monitoring point for the calibration was a shielded air temperature sensor located near the middle of the test cell. We also monitored a number of other variables to help provide more detailed insight into thermal performance. These

included the temperature of the air gap and temperature of the water in the heat exchanger. We also installed two heat flux sensors to characterize the flow of energy into and out of the wall assembly.

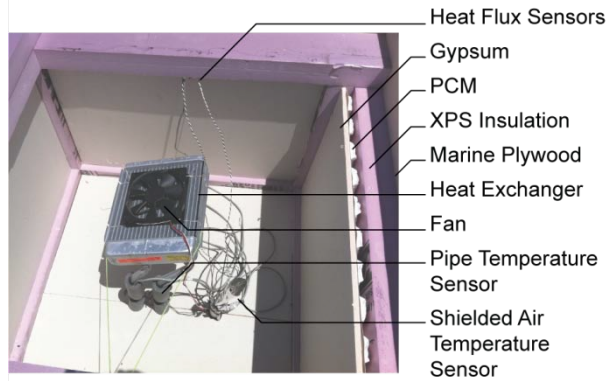


Figure 5 Test cell interior



Figure 6 The test cells in place

We monitored weather conditions for model calibration. At the site of the test cell, we monitored global horizontal solar radiation, air temperature, and relative humidity. The interval for all variables monitored on site was 5 minutes, with all measurements being recorded simultaneously. Nearby airport weather data from the Oakland Airport weather station were used as a reference for wind speed and dewpoint.

ENERGYPLUS MODEL

We built an EnergyPlus model of the test cell containing a single zone and using the same construction for all six surfaces (see Figure 7). Since the test cells were located on a roof painted with a reflective surface, an exterior shading object with high surface reflectivity was included 7 inches below the box. In order to simulate PCM, the ConFD heat balance algorithm was used for every simulation. For

comparison with the physical model, the EnergyPlus model was configured to report mean air temperature at every timestep (ie, every minute), and it was set to run from July 15 through August 7, which was the period of time for which we had good quality data for calibration. This established the metric for assessing the quality of a particular model being run: a good model would produce temperature data close to the temperature data recorded in the physical model.

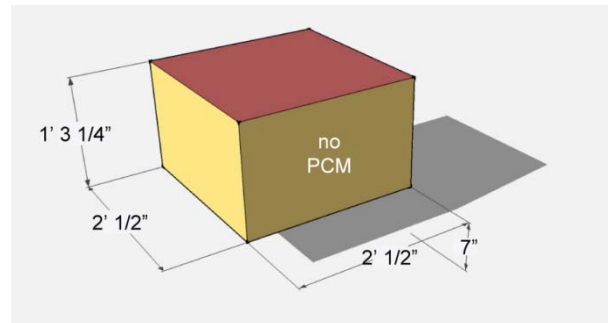


Figure 7 EnergyPlus test cell model

For the weather file used in the simulation, we modified the current EnergyPlus Weather (EPW) file containing Typical Meteorological Year data. We changed the values in this file to match the values recorded within the calibration period. Columns that would not impact this analysis were not changed (eg, illuminance was not changed). The columns changed to match measured data were dry bulb temperature, relative humidity, global horizontal radiation, dewpoint, and wind speed. Early tests also showed that direct normal radiation and diffuse radiation would have a significant impact on the model. We did not have measured data for these variables. Instead, we made the assumption that observed patterns in global horizontal radiation can predict the diffuse and direct radiation components.

Using the RMSE method described below, we identified which day in the EPW file most closely matched the global horizontal radiation measured for a particular day in the calibration period, and then used the direct and diffuse components from that EPW day as the actual data. A cloudy day on August 4 produced a pattern of solar radiation very different from any day in the weather file (ie, the squared sum of errors between the actual recorded radiation and the best fit day of radiation data in the weather file was significantly higher than the error for any of the other days), resulting in predictions for diffuse and direct normal solar radiation for that day that were likely poor. We therefore eliminated that day from the calibration process.

CALIBRATION

The goal of the calibration process was to develop an accurate technique for modeling the thermal behavior of PCM. Since an energy model is built to represent a piece of a complex world, it is, by necessity, an abstraction. A model contains many approximations, assumptions, and simplifications (Maile 2010). Calibration of the model against measured data allows sets of these inputs to be tested, yielding sets of inputs that are deemed to be more accurate than others.

CALIBRATION TOOLS

In order to assess how closely one data series matched another, we developed a tool to automate the process of computing the root mean squared error (RMSE) for each set of model results. Visually, a lower RMSE results in a graph of simulated temperature data that matches the actual data very closely (ie, the error between the simulated and predicted is very small). Mathematically, we define RMSE as:

$$RMSE = \sqrt{\frac{\sum(x_i - y_i)^2}{n}}$$

where:

n is the number of data points

y_i is the actual value for the i^{th} data point

x_i is the simulated value for the i^{th} data point

This tool was inserted into the modeling workflow as a script called from the EnergyPlus batch file. This script took the actual temperature data and calculated the RMSE after each run, saving the RMSE in the .eso output file.

We used two methods of automating the search for the most accurate model. Each method used GenOpt, a generic optimization platform designed to control an external simulation in search of a set of simulation parameters that minimize a cost function. In this study, we used the calculated RMSE value as the cost function, which effectively set up GenOpt to search for a set of parameters that resulted in the smallest error between simulated temperatures and actual temperatures.

One method this study used to search for an optimal set of parameters was a Generalized Pattern Search (GPS), using the Hooke-Jeeves implementation in particular. Using this algorithm, GenOpt systematically varies each parameter from an initial value, looking for whether a small increase or decrease in the parameter will lower the cost. As new points of lower cost are found, the algorithm searches again from the lowest point identified. GPS runs until no incremental changes

lower the cost. This ensures that GPS finds a local optimum in the cost function. However, since the cost function is produced by energy simulation, it is discontinuous and therefore subject to local minima at locations that may not be the same as the global minimum.

In order to ensure that the global minimum was identified, this study also utilized a parametric sweep search method. We used Genopt to run a set of every possible combination of selected parameters, recording the cost for each simulation. Since all combinations are covered, the parameter sweep will be more likely to indicate what combination of parameters might be close to the global minimum. We then used GPS to search around the optimal point selected by the parameter sweep.

The drawback of using a parameter sweep was computational expense: for each additional parameter studied, the total number of simulations increased by a factor of the number of values tested for that parameter. For example, to test five values for each of five parameters, the total number of combinations was $5 \times 5 \times 5 \times 5 \times 5$ or 3125. If one more parameter of 6 values were added, the total increases to 18,750. The increase is exponential relative to the number of parameters selected.

Because of the large number of simulations required for a parameter sweep search, we utilized the Amazon Elastic Compute Cloud (EC2) in order to process a large number of simulations quickly. In the process of completing each set of calibrations, this study recorded over 400,000 individual simulation runs.

CALIBRATION OF MODEL WITHOUT PCM

The calibration was done in two stages. The first step in the calibration process was to calibrate the energy model representing test cell without PCMs. This step was necessary due to the uncertainty of modeling assumptions associated with all aspects of the test cell simulation other than the PCM. Calibration of the control allowed the effect of the PCM to be isolated.

Once the model was running successfully with an initial set of assumptions, five parameters were selected in order to calibrate the model to the actual results:

- U-value of insulation
- Specific Heat of gypsum
- Solar absorptivity of exterior paint
- Infiltration
- Internal mass

After running an initial parameter sweep, it was discovered that the optimal solutions were occurring at the edge of the parameter ranges, indicating that the

optimal solution could be outside the ranges selected. Expanding the parameter ranges revealed that the optimal values for specific heat and insulation were much lower than reasonable. Careful study of the simulated temperature data revealed a potential shift between the actual data and the simulated data. One possible explanation for this discrepancy is that weather data is reported for a particular hour, but is not necessarily averaged over that hour. In order to compensate for time shift error, the timestamps of the actual data were shifted. A time shift of 45 minutes produced a better fit for the data. Repeating the parameter search produced values for the parameters that made more sense with the test cell construction materials. Ultimately, simulated and measured interior air temperatures matched closely (see Figure 8).

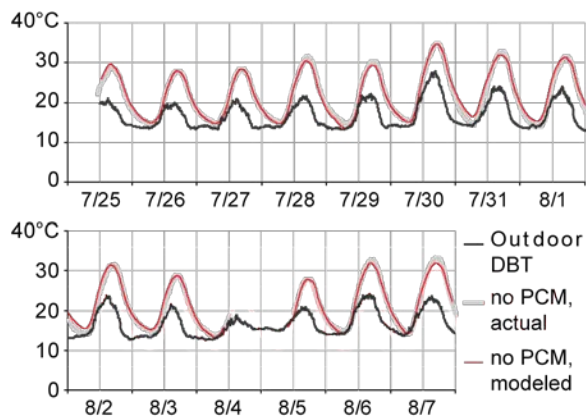


Figure 8 Comparison of calibrated model predicted interior temperature with actual measured interior temperature for test cell without PCM

CALIBRATION OF MODEL WITH PCM

Finally, the thermal characteristics of the PCM were calibrated using the test cell containing PCM. Since these test cells were constructed identically, the only difference between each test cell is the addition of PCM. We added the objects necessary to model PCM, and then conducted a parameter search for an optimal combination of the PCM enthalpy curve and other PCM thermal properties described above. We studied different options for modeling the geometry of this PCM product. Since the PCM on a sheet of the product covers about 4/9 of the surface area, one option we studied was to subdivide each surface into a PCM part and a part without PCM (see Figure 9). We also studied a model where the PCM covered a smaller area, and a model where the PCM covered the entire area. In each case, the thickness of the PCM was adjusted so that the total mass of PCM was the same, and equivalent to the actual mass of PCM in the test cell.

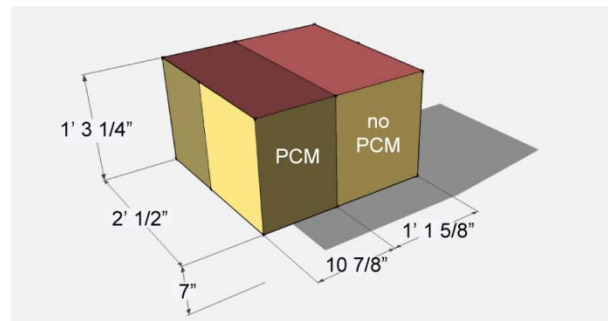


Figure 9 EnergyPlus test cell model showing subdivision of surfaces

For each unknown coordinate on the enthalpy curve (T2, E2, T3, E3, and E4), we selected ranges based on the enthalpy curve provided by the manufacturer, and chose to search five points within each range. We similarly selected values for the two conductivity parameters.

We first ran a parameter sweep using GenOpt. This yielded an optimized enthalpy curve that contained points at the edge of the parameter domain (see figure 10).

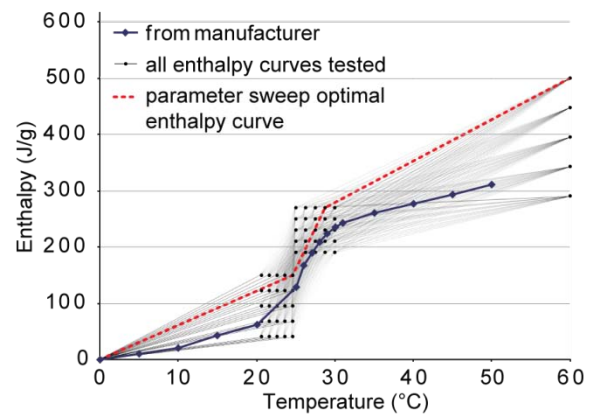


Figure 10 Enthalpy curve from the manufacturer, all enthalpy curves analyzed during parameter sweep, and optimal enthalpy curve selected by parameter sweep

Once the initial parameter search was completed, we ran GPS starting at the optimal set of parameters, expanding ranges of enthalpy values since the parameter sweep found optima at the high end of the parameter range for those values. While in the control optimization this indicated an error with the model, the following graph shows why this made sense in this situation. The temperature range represented in the dataset is limited to about 16°C to 31°C, so the enthalpy curve was calibrated in that range. The values outside that range were not tested, and so the slope of the line

segment outside that range is meaningless. We can therefore cut those line segments at the edges of the range and assign a default slope for the line segments outside this range. Using the slope of the enthalpy curve from the manufacturer, we can arrive at a new enthalpy curve that is calibrated within the range of 16°C to 31°C. The difference in enthalpy from the low end of the range to the high end matches the difference reported in the manufacturer’s laboratory test within 2% (see Figure 11).

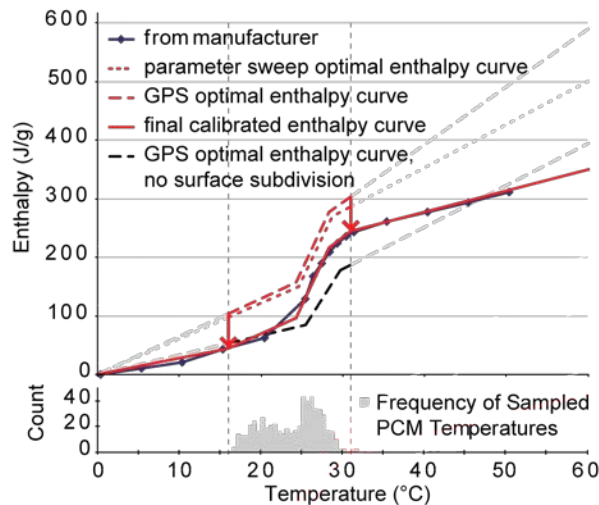


Figure 11 The final calibrated enthalpy curve is a combination of the GPS optimal enthalpy curve within the range of temperatures sampled during the calibration, and the laboratory provided enthalpy curve for points outside the calibration range. Also shown is the GPS optimal enthalpy curve selected if the PCM is modeled as a continuous sheet of PCM, rather than subdividing it into part PCM and part no PCM.

To summarize, Table 1 shows calibrated values for the PCM parameters studied. The simulated interior air temperatures matched the monitored temperatures closely (see Figure 12).

Table 1 Final calibrated values

CALIBRATED PARAMETER	CALIBRATED VALUE
Enthalpy Curve (C, J/kg)	{ (0, 0), (16, 45000), (24.25, 97000), (28.275, 217000), (31, 245000), (60, 350000) }
Conductivity (W/m-K)	0.1
Temperature Coefficient for Thermal Conductivity (W/m-K ²)	-0.0105

Modeling Approach	Subdivide the PCM surface into two areas. The PCM area should cover 4/9 of the total surface area. Constructions for each area should be identical except that the PCM material should only be included in the PCM area.
-------------------	--

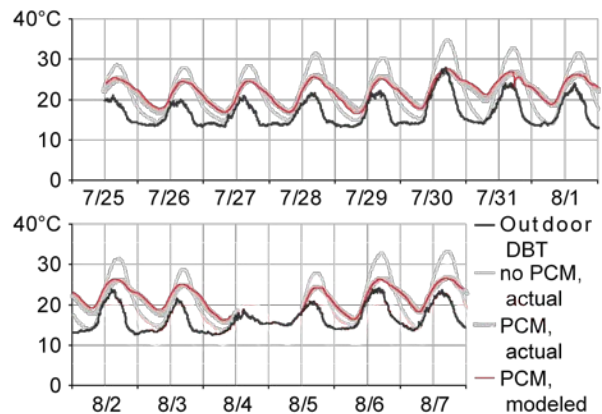


Figure 12 Comparison of calibrated model predicted interior temperature with actual measured interior temperature for test cell with PCM

DISCUSSION

The process of calibration used in this study required (a) quantifying how accurately a particular model predicts thermal behavior in the real world, (b) comparing models to identify which provide the best predictions, and (c) judgment regarding which abstractions are more likely to be representative of the real world. The automated search for optimal sets of parameters was essential to the process, but so too was the judgment to know when an iteration in the calibration process required variation of a parameter orthogonal to the parameterized domain.

While the use of judgment may seem antithetical to an idealized process of calibration, we view these techniques as complimentary. When incorrect assumptions have been made and not parameterized, the calibration process may converge at incorrect and/or nonsensical values that partially compensate for the incorrect assumptions. The modeler uses judgment to identify this behavior and to choose a response.

This kind of judgment helped confirm the best modeling approach for this PCM product. The results show better predictions (ie, lower RMSE) when the surface is subdivided compared with when it is modeled as a continuous surface. To confirm this result, we looked at the optimized solution for the approach of modeling the complete surface. This approach requires

very different parameter values in order to achieve the closest fit to the data. The corresponding enthalpy curve is shown in Figure 11: it shows a 31% smaller increase in enthalpy within the calibration range. Furthermore, the optimal conductivity value is much larger than that identified by the subdivided surface calibration. Our interpretation for this effect is that thermal bridging needs to be considered. In the physical model, some heat will be transferred through the PCM sheet product without affecting the PCM since it can travel across the parts that are not covered by PCM. If the model does not include these highly conductive paths, then the model underestimates heat transfer through the PCM. The calibration attempts to compensate for this by increasing the thermal conductivity of the PCM, which in turn yields a suspect calibrated enthalpy curve.

While the convergence behavior yields some insights into accurate modeling approaches, it may also be compensating for systemic inaccuracies. This would be the case if this PCM product exhibited differences between freezing and melting behavior. Hysteresis is not modeled by EnergyPlus, so it is possible that the optimized modeling values may be compensating for hysteresis, for instance by yielding a less steep enthalpy curve within the phase transition zone

CONCLUSION

More generally, we have shown that EnergyPlus has the capability of simulating the behavior of phase change material quite closely. This study was performed using test cells to facilitate experimental control, but the partial freezing and partial melting behavior of the PCM in the test cells would likely be present in building applications as well. The next step for this research is to study the performance of the PCM product in a real building. A similar research design could be used, such as selection of two similar rooms, with PCM installed in one, and the other used as a control. While studying spaces in a functioning building will add complexity to the experimental design, it will be critical to demonstrate the product's effectiveness in meeting its energy reduction and thermal comfort goals.

ACKNOWLEDGMENT

The authors thank Project Frog for funding the research, and Ash Notaney in particular for his support and for asking the questions that the study sought to answer. The authors also thank Fred Bauman and the Center for the Built Environment for lending some of the monitoring equipment used in the project.

REFERENCES

Dutil, Y., D. Rousse, S. Lassue, L. Zalewski, A. Jaoulin, J. Virgone, F. Kuznik, K. Johannes, J. Dumas, J.

Bedecarrats, A. Castell, and L. Cabeza. 2014. "Modeling phase change materials behavior in building applications: Comments on material characterization and model validation." *Renewable Energy* 61: 132-135.

Jin, X., M. A. Medina, X. Zhang. 2013. "On the importance of the location of PCMs in building walls for enhanced thermal performance" *Applied Energy* 106: 72-78.

Kissock, K., and S. Limas. 2006. "Diurnal Load Reduction Through Phase-Change Building Components." *ASHRAE Transactions* 112:509-517.

Kosny, J., T. Stovall, S. Shrestha, D. Yarbrough. 2010. "Theoretical and experimental thermal performance analysis of complex thermal storage membrane containing bio-based phase-change material (PCM)." Proceedings of *Thermal Performance of Exterior Envelopes of Whole Buildings XI*, Florida, USA.

Kuznik, F., D. David, K. Johannes, JJ. Roux. 2011. "A review on phase change materials integrated in building walls." *Renewable and Sustainable Energy Reviews* 15: 379-391.

Medina, M, J. B. King, M. Zhang. 2008. "On the heat transfer rate reduction of structural insulated panels (SIPs) outfitted with phase change materials (PCMs)" *Energy* 33: 667-678

Maile, T., M. Fischer, J. Haymaker, and V. Bazjanac. 2010. "Formalizing approximations, assumptions, and simplifications to document limitations in building energy performance simulation." Center for Integrated Facility Engineering Working Paper 126. Stanford University.

Pedersen, C. O. 2007. Advanced zone simulation in EnergyPlus: incorporation of variable properties and phase change material (PCM) capability, in: Proceedings: Building Simulation 2007. IBPSA, Beijing, China.

Silva T., R. Vicente, N. Soares, and V. Ferreira. 2012. "Experimental testing and numerical modeling of masonry wall solution with PCM incorporation: A passive construction solution" *Energy and Buildings* 49: 235-245.

Tabares-Velasco, P. C., C. Cristensen, and M. Bianchi. 2012. "Verification and validation of EnergyPlus phase change material model for opaque wall assemblies." *Building and Environment* 54: 186-196.